An SIDM simulation study of the merging cluster El Gordo and its tension between the post collision DM density profiles and weak lensing constraints

R. Valdarnini (SISSA)

Valencia workshop on the Small Scale Structure of the Universe and SIDM, June 9-20 2025

ESO/SOAR/NASA

- Major mergers between galaxy clusters are very energetic events $\left(E \sim 10^{64} ergs,\ M_1 \sim M_2 \sim 10^{15}\,\mathrm{M}_\odot,\ \mathrm{V_{rel}} \sim 2,000\mathrm{Km/s}\right)$ and can be considered natural laboratories which provide a wealth of informations (X-ray, opt, SZ, WL…) about the physics of the ICM and the nature of DM

An extreme example of a high redshift major cluster merger is the EL Gordo cluster (ACT-CL 10162-4915) . This cluster has the largest SZ effect in the ACT survey

Such a massive merger at high redshits is a serious challenge to ΛCDM cosmology (Asencio+21, Kim+21)

MAIN MORPHOLOGICAL FEATURES OF El GORDO CLUSTER

- Two clusters: northwestern (NW) and southeastern (SE)
- NW is the primary and SE the secondary cluster

- $d_{DM}^{proj} \sim 700\,\mathrm{kpc}$ $\quad M_1 \sim 1.4 \cdot 10^{15}\,\mathrm{M}_\odot$ $\quad z \sim 0.87$
- $L_X \sim 2 \cdot 10^{45}\,\mathrm{ergs}^{-1}$ $\quad M_1/M_2 \sim 2$ $\quad V_{\mathrm{infall}} \sim 2,500\,\mathrm{km\ s}^{-1}$

- Strong X-ray peak in the SE cluster , with two tails
- NW emission very weak
- There are large offsets between the different centroids:
  - $d_{SZ-NW} \sim 150\,\mathrm{kpc}$
  - $d_{X-BCG}^{SE} \sim 70\,\mathrm{kpc}$
  - $d_{X-DM}^{SE} \sim 100\,\mathrm{kpc}$
- At variance with what expected from dissipative arguments (and the Bullet Cluster) here the X-ray peak is not trailing the SE DM peak but is leading the mass peak- Moreover the BCG as well is offset from the DM centroid

Because of its many unusual properties El Gordo has been the subject of many N-body/hydro simulation studies (Donnert 14, Molnar & Broadhurst 15, Zhang + 15, RV24)

Interestingly, two lensing papers (Diego+20, Kim+21) consistently give mass lensing estimates for the NW and SE clusters lower than previously reported $\sim (60 - 30\%)$

This is in tension with Zhang+15, who argue that El Gordo simulations with a total cluster mass smaller than $\sim 3 \cdot 10^{15}\,\mathrm{M}_{\odot}$ will produce an X-ray emission much lower than observed

In light of these WL mass estimates it is thus an open issue if N-body/hydro simulations can reproduce the observed X-ray morphology.

I will present here recent findings from a detailed simulation study (RV 2024, A&A), of the merging cluster El Gordo. For the hydro part it is used an improved version of SPH (Integral SPH) which has been already tested in simulations of merging clusters (RV+Sarazin 21). We tested a variety of merging initial conditions in order to find which is the one that can best reproduce the observed twin tailed X-ray morphology and mass centroid offsets of El Gordo

The layout of the talk is the following :

- Initial condition (IC) set up
- Search of the optimal merger model
- Mergers with SIDM
- Conclusions

INITIAL CONDITION SET UP

We study collisions between a primary of mass M_1 and a secondary with mass M_2. The cluster mass is defined as the mass M_{200} within the radius r_{200} , where

$$M_\Delta = \frac{4\pi}{3}\Delta\rho_c(z)r_\Delta^3$$

We introduce the mass ratio $q = M_1/M_2$, which is a fundamental collision parameter

To construct the initial conditions of our merging simulations we first perform a particle realization of two individual halos in hydrostatic equilibrium . Each halo consists of DM , gas and (eventually) a star component

DM HALOS

We adopt a truncated NFW profile (Kazantzidis+04, K04)

$$\begin{cases} \rho_{DM}(r) = \dfrac{\rho_s}{r/r_s(1+r/r_s)^2}, & 0 \le r \le r_{200}, \\ \rho_{DM}(r) = \rho_{DM}(r_{200})(r/r_{200})^{\delta} \exp -\left(\dfrac{r-r_{200}}{r_{decay}}\right) & r_{200} < r < r_{max} \end{cases}$$

For the concentration parameter c we use the Duffy+08 relation

DM positions are assigned by first evaluating $M_{DM}(<r)$ and then inverting

$$\begin{cases} q(r) = M_{DM}(<r)/M_{DM}(<r_{rmax}) = y \\ y \in [0,1] \end{cases}$$

For the DM particle velocities we compute

$$\begin{cases} \rho_m(r) &= 4\pi \int_0^{\Psi(r)} f_m(\mathcal{E}) \sqrt{2[\Psi(r) - \mathcal{E}]}\, d\mathcal{E}, \\ f_m(\mathcal{E}) &= \frac{1}{\sqrt{8}\pi^2} \left[\int_0^{\mathcal{E}} \frac{d^2\rho_m}{d\Psi^2} \frac{d\Psi}{\sqrt{(\mathcal{E}-\Psi)}} \right. \\ m &= DM,\ star \end{cases}$$

For a particle at position r we then draw random pair $(f, \mathcal{E})$ where

$$\begin{cases} \Psi(r) &= -\Phi(r) \\ \mathcal{E} &= \Psi - v^2/2 \end{cases}$$

and use a rejection method to obtain $v = \sqrt{2[\Psi(r) - \mathcal{E}]}$

BARYONIC HALOS

The initial gas distribution of each halo is assumed to follow either a Burkert profile, as in Zhang+15, or a non-isothermal β-model

$$\begin{cases} \rho_{gas}(r) = \dfrac{\rho_0}{(1+r/r_c)[1+(r/r_c)^2]}\,, & 0 \le r \le r_{200}\,, \\ \rho_{gas}(r) = \dfrac{\rho_0}{(1+r/r_c)^{-3\beta/2}}\,, & \beta = 2/3\,, \\ \rho_{gas}(r) = \rho_{DM}(r)\dfrac{\rho_{gas}(r_{200})}{\rho_{DM}(r_{200})} & r_{200} < r < r_{max} \end{cases}$$

Assuming hydrostatic equilibrium, we construct cluster profiles by integrating

$$T(r) = \frac{\mu m_p}{k_B}\frac{G}{\rho_{gas}(r)}\int_r^\infty \frac{\rho_{gas}(t)}{t^2} M_{tot}(<t)dt\ ,$$

STELLAR COMPONENT

For some of our merging runs we consider halos with a stellar component. This is to mimick the presence of a BCG

We adopt the following stellar density profile (Merritt+06)

$$
\begin{cases}
\rho_\star(r) & = & \rho_e \, \exp\left\{-d_{n_s}\left[(r/r_e)^{1/n_s}-1\right]\right\} & , \\
d_{n_s} & \sim & 3n_s - 1/3 + 0.0079/n_s & n_s = 6 \ , \\
r_e & = & 60\,\mathrm{kpc} & , \\
\log_{10} M_{\star,BCG} & \sim & 0.38[\log_{10}(M_{500}) - 14.5]
\end{cases}
$$

where the BCG mass ($\sim 10^{12} M_\odot$) is determined from Kravtsov+18

Positions and velocities are assigned to particles as in the realization of DM halos

INITIAL MERGER KINEMATIC

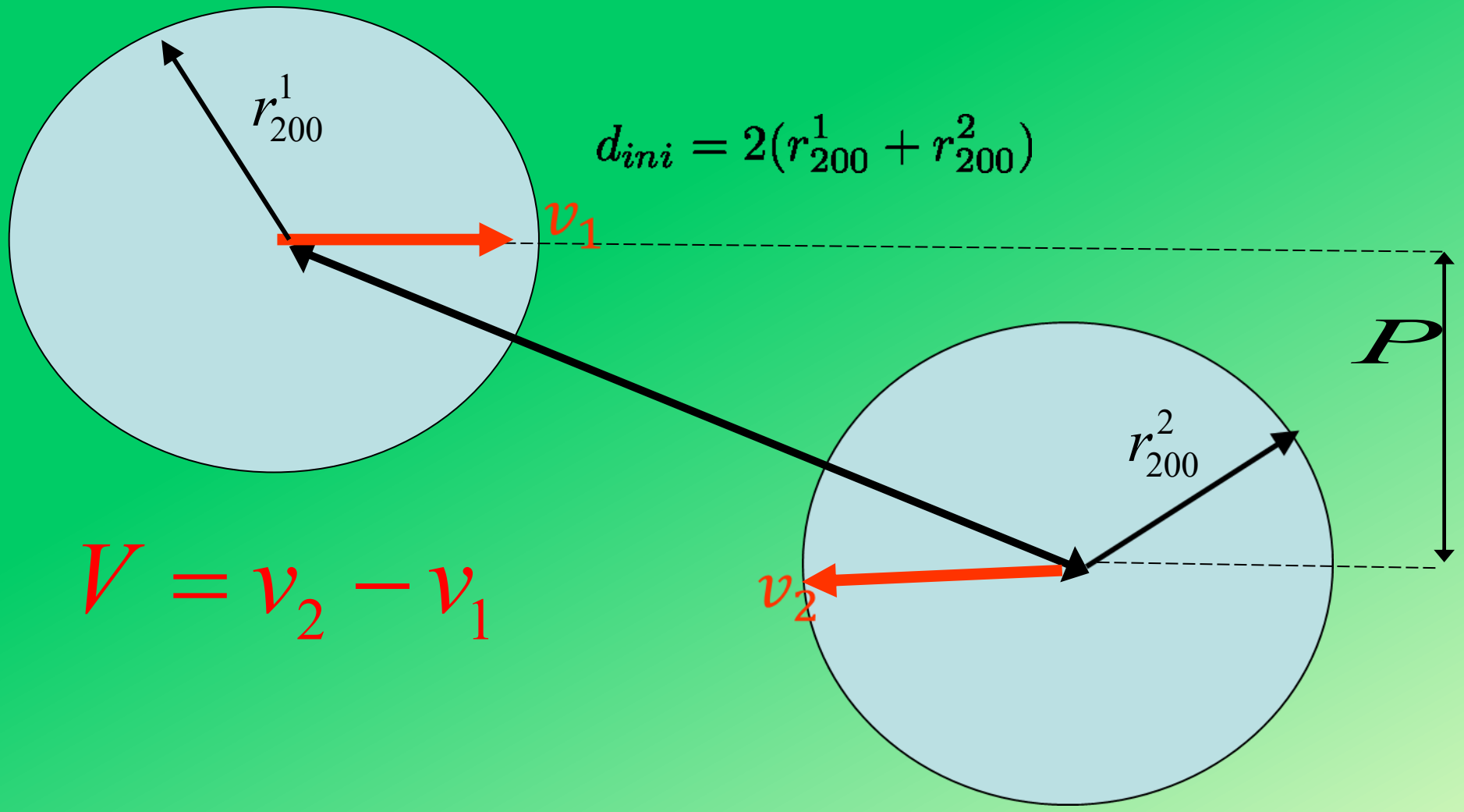

Each cluster consists of a gas+DM [+star] halo

SIMULATION STRATEGY

A merging simulation of the El Gordo cluster must be able to satisfy the following constraints:

- Projected distance between the mass centroids: $d_{DM} \sim 700\,\mathrm{kpc}$
- Twin-tailed X-ray morphology
- $L_X \sim 2 \cdot 10^{45} h_{70}^{-2}\,\mathrm{ergs}^{-1}\ [0.5-2]\,\mathrm{keV}$
- Offsets of DM to BCG, X-ray and SZ centroids

We adopt the same collision geometry of Zhang+15 and construct a grid of simulations by varying the primary's mass, the collision parameters V and P, the gas density profile of the primary

This is the set of merging simulations with different collision parameters

Zhang+15

Table 1: IDs and initial collision parameters of the off-axis merger simulations.
[a]

Model	$M_{200}^{(1)}$ [$M_\odot$]	r_{200} [Mpc]	q	V [kms^{-1}]	P [kpc]	(f_{g1}, f_{g2})	gas profile
B_1	2.5×10^{15}	2.02	3.6	2500	800	(0.05,0.1)	Burkert
A_1	1.3×10^{15}	1.63	2.0	3000	300	(0.1,0.1)	Burkert
Bf	1.6×10^{15}	1.74	2.32	2500	600	(0.1,0.1)	β-model
Bg	1.6×10^{15}	1.74	2.32	2000	600	(0.1,0.1)	β-model
Bh	1.6×10^{15}	1.74	2.32	1500	600	(0.1,0.1)	β-model
Bk	1×10^{15}	1.5	1.54	1500	600	(0.1,0.1)	β-model
Bl	1×10^{15}	1.5	1.54	2000	600	(0.1,0.1)	β-model

Notes. [a] Columns from left to right: ID of the merging model, halo mass $M_{200}^{(1)}$ of the primary , cluster radius r_{200} at which $\Delta = 200$, primary-to-secondary mass ratio $q = M_1/M_2$, initial collision velocity, collision impact parameter, primary and secondary cluster gas mass fractions f_g at r_{200}, adopted model for the gas density profile of the primary. The last row refers to the head-on mergers.

For a given set of collision parameters $\{M_1, q, V, P\}$ we explore mergers with an initially different gas core radius of the primary. Each simulation is identified by a subscript added to the merger model

Table 2: IDs of the merger simulations with initial merging parameters as given by the corresponding merger models of Table 1. For each merger model the additional subscripts refer to simulations with an initially different gas core radius r_c of the primary. For each simulation we report the value of r_c and that of the ratio $\zeta = r_s/r_c$, where r_s is the NFW scale radius of the primary.

0.8

Model: $\{M_1, r_s,\ q,\ P,\ V\}$	merger simulation ID					
Bf: $\{1.6 \cdot 10^{15}, 0.696,\ 2.32,\ 600,\ 2,500\}$	Bf_rc29	Bf_rc26	Bf_rc22	Bf_rc20	Bf_rc17	Bf_rc14
r_c $(\zeta = r_s/r_c)$	290 (2.4)	260 (2.67)	217 (3.2)	200 (3.44)	174 (4.)	145 (4.81)
Bg: $\{1.6 \cdot 10^{15}, 0.696,\ 2.32,\ 600,\ 2,000\}$	Bg_rc29	Bg_rc23	Bg_rc20	Bg_rc17	Bg_rc14	
r_c $(\zeta = r_s/r_c)$	290 (2.4)	232 (3)	200 (3.437)	174 (4)	145 (4.81)	
Bh: $\{1.6 \cdot 10^{15}, 0.696,\ 2.32,\ 600,\ 1,500\}$	Bh_rc29	Bh_rc22	Bh_rc20	Bh_rc17	Bh_rc16	Bh_rc14
r_c $(\zeta = r_s/r_c)$	290 (2.4)	217(3.2)	200(3.44)	174(4.)	160(4.37)	145(4.81)
Bk: $\{1. \cdot 10^{15}, 0.574,\ 1.54,\ 600,\ 1,500\}$	Bk_rc19	Bk_rc18	Bk_rc17	Bk_rc15	Bk_rc14	Bk_rc12
r_c $(\zeta = r_s/r_c)$	191 (3.)	179 (3.206)	167 (3.43)	155 (3.7)	143 (4)	119 (4.81)
Bl: $\{1. \cdot 10^{15}, 0.574,\ 1.54,\ 600,\ 2,000\}$	Bl_rc24	Bl_rc21	Bl_rc19	Bl_rc18	Bl_rc17	Bl_rc14
r_c $(\zeta = r_s/r_c)$	240 (2.39)	215 (2.67)	191 (3.0)	179 (3.207)	167 (3.43)	143 (4)

$\zeta = r_c / r_s$

Best-fit models: Bf_rc20, Bg_rc20 and Bl_rc24

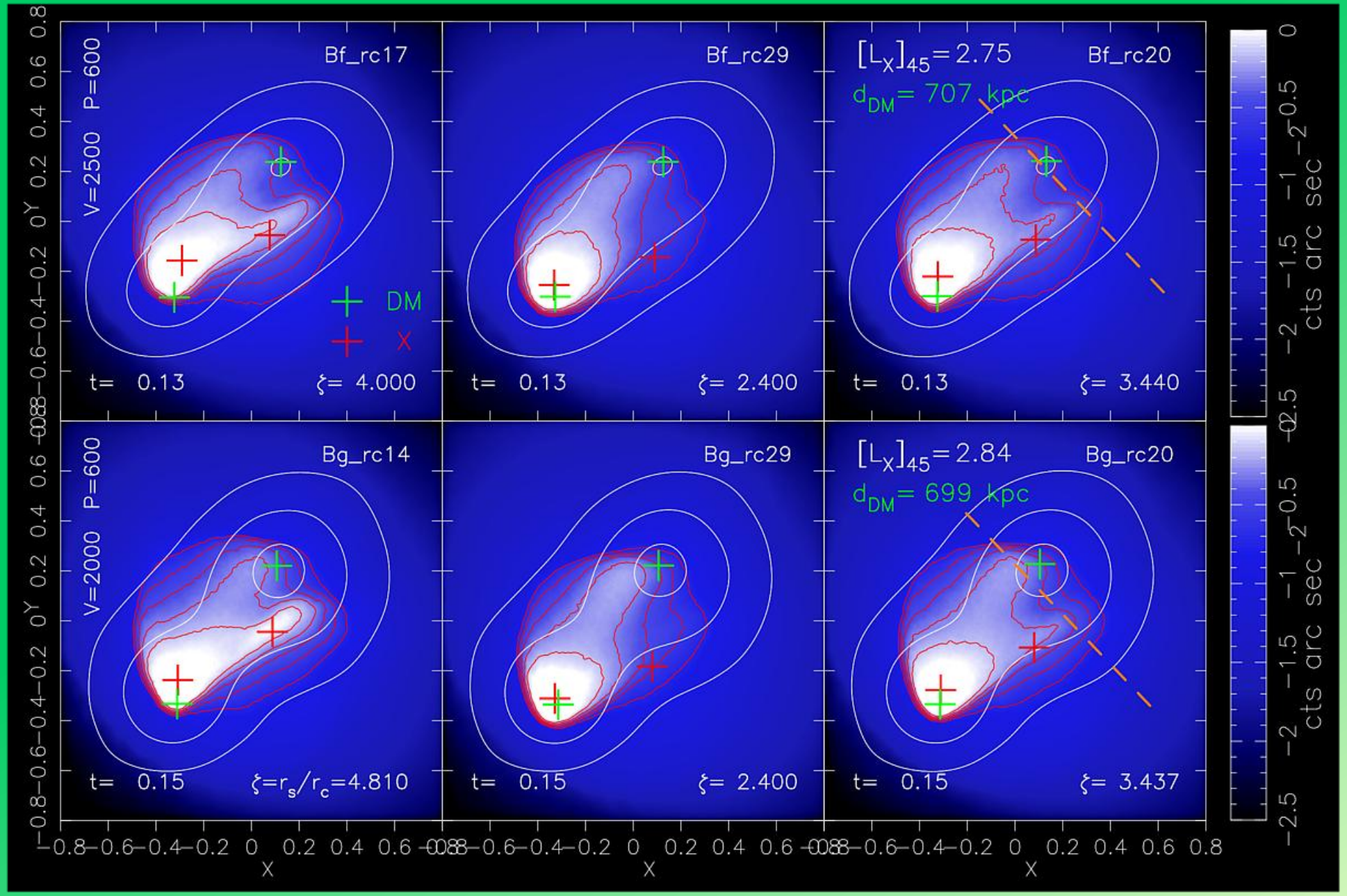

$\zeta = r_c / r_s$

t[Gyr]=time since pericenter

CONCLUSIONS (standard CDM):

The twin-tailed X-ray morphology can be reproduced in merging simulations of El Gordo which satisfy

$$\begin{cases} 10^{15}\,\mathrm{M}_\odot & \lesssim & M_1 & \lesssim 1.6\cdot 10^{15}\,\mathrm{M}_\odot \\ M_2 & \sim & 6.5\cdot 10^{14}\,\mathrm{M}_\odot & \\ 2,000\,\mathrm{km\ s^{-1}} & \lesssim & V & \lesssim 2,500\,\mathrm{km\ s^{-1}} \\ 600\,\mathrm{kpc} & \lesssim & P & \lesssim 800\,\mathrm{kpc} \end{cases}$$

Models Bf_rc20, Bg_rc20 and Bl_rc24 appear to give the best match to the whole data

However these simulations leave open the issue of the centroid positions (in the standard collisionless CDM scenario). Moreover, in these models the relative radial velocity V_r between the two galaxy groups is sistematically higher ($\sim 1,000\,\mathrm{km\ s^{-1}}$) than observed ($V_r^{obs} \sim 600\,\mathrm{km\ s^{-1}}$)

RESULTS FROM SIDM MERGING SIMULATIONS OF El GORDO

We model DM interactions according to a Monte Carlo method – we assume isotropic and elastic scattering

We perfom three SIDM runs for each of the two merger models Bf_rc20 and Bl_rc24 (plus BCGs): XDBf_rc20 and XDBl_rc24

For the DM cross section we considered the following values : $\sigma_{DM}/m_X = 1,\ 2,\ 5\,\mathrm{cm}^2\mathrm{gr}^{-1}$

CENTROIDS POSITIONS

+: DM +: X-ray +: SZ ★ : BCG

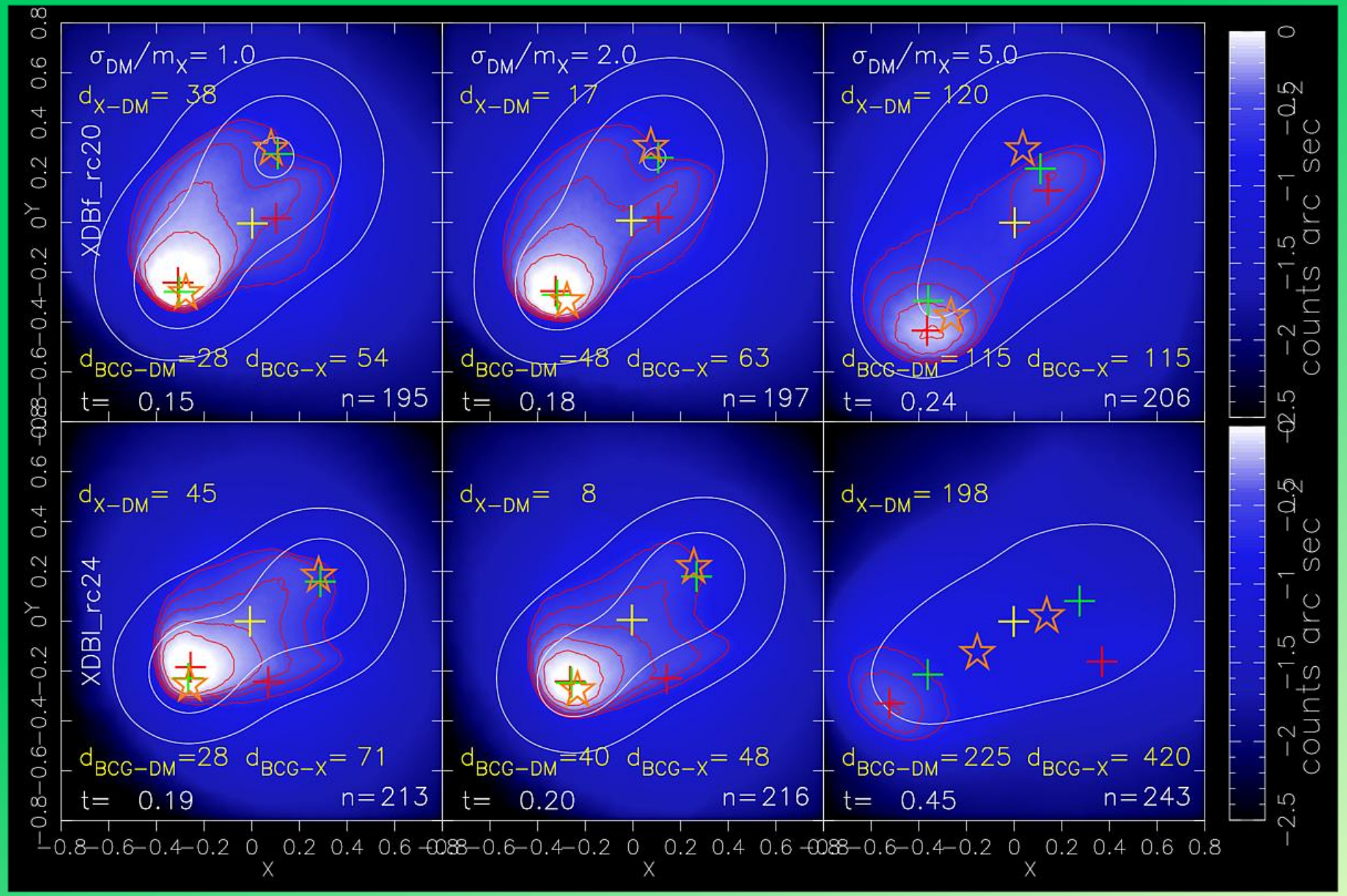
σDM/mX= 1.0
dX−DM= 38
dBCG−DM=28 dBCG−X= 54
t= 0.15 n=195
σDM/mX= 2.0
dX−DM= 17
dBCG−DM=48 dBCG−X= 63
t= 0.18 n=197
σDM/mX= 5.0
dX−DM= 120
dBCG−DM=115 dBCG−X= 115
t= 0.24 n=206
XDBf_rc20
dX−DM= 45
dBCG−DM=28 dBCG−X= 71
t= 0.19 n=213
dX−DM= 8
dBCG−DM=40 dBCG−X= 48
t= 0.20 n=216
dX−DM= 198
dBCG−DM=225 dBCG−X= 420
t= 0.45 n=243
XDBl_rc24
X
Y
counts arc sec

MAIN RESULTS

- Because of DM dissipation during the collision: shallower DM potentials: → post-pericenter X-ray structures can more easily escape from DM potential wells
- X-ray peak now leading the SE DM centroid

- Note: t is the elapsed time since pericenter until when $d_{DM} \sim 700\,\mathrm{kpc}$

- The time t increases as $\sigma_{DM}/m_X \to 5\,\mathrm{cm}^2\mathrm{gr}^{-1}$ because of the slowdown of DM bulk velocities due to DM dissipation

- The separations between the different mass centroids are locked to d_{DM}, which fixes the present epoch through the dynamic when $d_{DM} \sim 700\,\mathrm{kpc}$

- As $\sigma_{DM}/m_X \to 5\,\mathrm{cm}^2\mathrm{gr}^{-1}$ only model XDBf_rc20 is able to match the observed offsets at t ~ 0.25 Gyr

- Model XDBl_rc24 ($10^{15} M_\odot$) has t ~ 0.45 Gyr and much higher offsets

-This implies that the SIDM model has no free parameters: only $\sigma_{DM}/m_X \sim 4 - 5\,\mathrm{cm}^2\mathrm{gr}^{-1}$ with $M_1 = 1.6 \cdot 10^{15}\,\mathrm{M}_\odot$ is able to match the observed separations

Because of the disruption of X-ray structures we now reconsider model XDBf_rc20 , but with larger gas core radii and gas fractions : XDBf_sa ($\sigma_{DM}/m_X = 5cm^2/gr$) and XDBf_sb ($\sigma_{DM}/m_X = 4cm^2/gr$)

Table 6: IDs and initial merger parameters of the two SIDM merging simulations [a].

Model	$M_\star^{(1)}[\mathrm{M}_\odot]$	$M_\star^{(2)}[\mathrm{M}_\odot]$	$N_\star^{(1)}$	$\varepsilon_\star[\mathrm{kpc}]$	$r_c^{\mathrm{prm}}[\mathrm{kpc}]$	ζ	$\sigma_{DM}/m_X[\mathrm{cm^2 gr^{-1}}]$	(f_{g1}, f_{g2})
XDBf_sa	2.2×10^{12}	1.6×10^{12}	16,785	9.5	406	1.7	5	(0.12,0.12)
XDBf_sb	2.2×10^{12}	1.6×10^{12}	16,785	9.5	290	2.4	4	(0.12,0.14)

Notes. [a] Columns from left to right: ID of the merging model, stellar mass of the BCG of the primary, the same mass but for the secondary, number of star particles for the primary, gravitational softening length of the star particles, gas core radius of the primary, dimensionless parameter $\zeta = r_s/r_c$, self-interacting DM cross section per unit mass, primary and secondary cluster gas mass fractions f_g at r_{200}. For the two SIDM merger models the collision parameters are those of model Bf in Table 1: $\{M_{200}^{(1)},\ q,\ V,\ P\} = \{1.6\cdot10^{15}\,\mathrm{M}_\odot,\ 2.32,\ 2,500\,\mathrm{km\ s^{-1}},\ 600\,\mathrm{kpc}\}$.

We only show results from model XDBf_sb

We compare the centroid positions with those obtained from data (Kim+21) : here we show their Fig. 6 , from which we extract X-ray emission, DM and BCG mass peak positions both for the SE and NW clusters

In the following mock X-ray map, these positions are indicated with filled circles, the color coding being the same of the associated crosses, which indicate the centroid location as have been extracted from the simulations

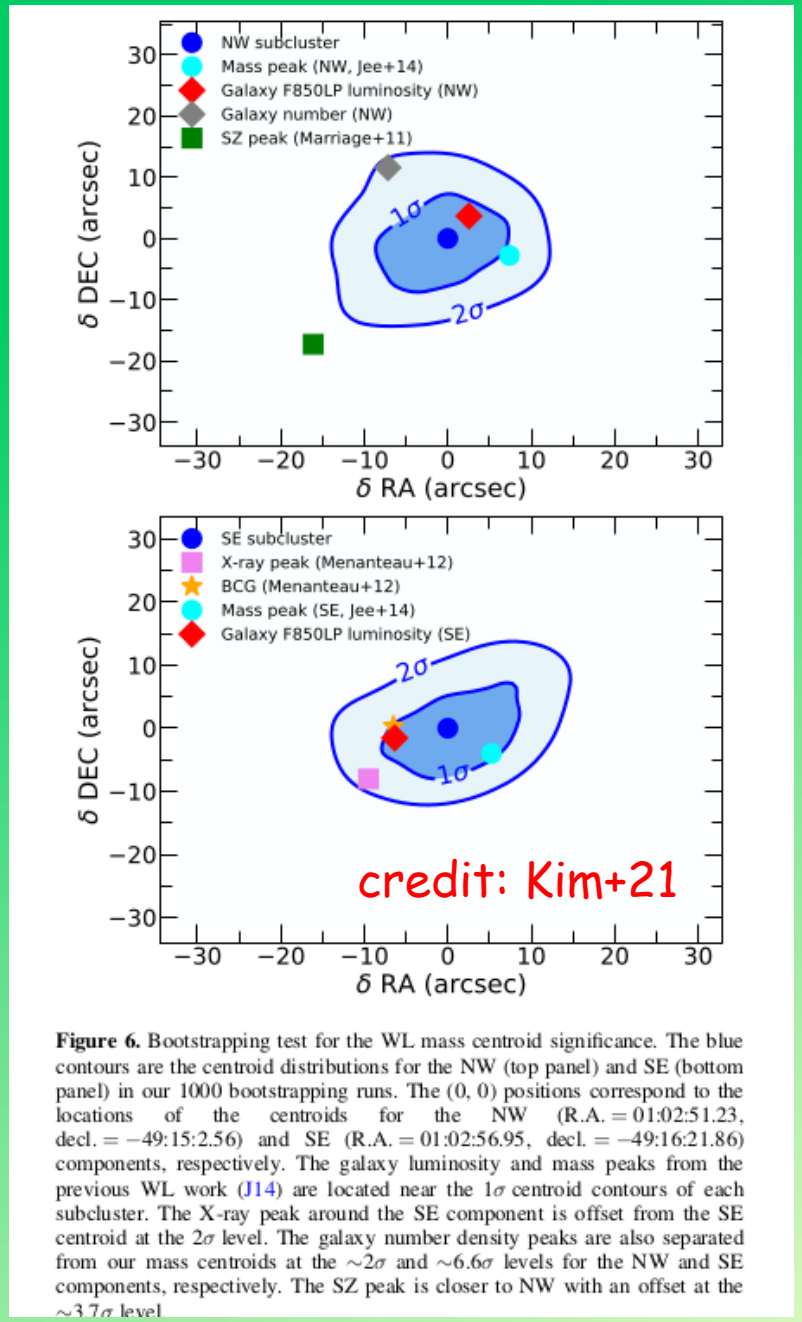

Figure 6. Bootstrapping test for the WL mass centroid significance. The blue contours are the centroid distributions for the NW (top panel) and SE (bottom panel) in our 1000 bootstrapping runs. The (0, 0) positions correspond to the locations of the centroids for the NW (R.A. = 01:02:51.23, decl. = −49:15:2.56) and SE (R.A. = 01:02:56.95, decl. = −49:16:21.86) components, respectively. The galaxy luminosity and mass peaks from the previous WL work (J14) are located near the 1σ centroid contours of each subcluster. The X-ray peak around the SE component is offset from the SE centroid at the 2σ level. The galaxy number density peaks are also separated from our mass centroids at the ∼2σ and ∼6.6σ levels for the NW and SE components, respectively. The SZ peak is closer to NW with an offset at the ∼3.7σ level

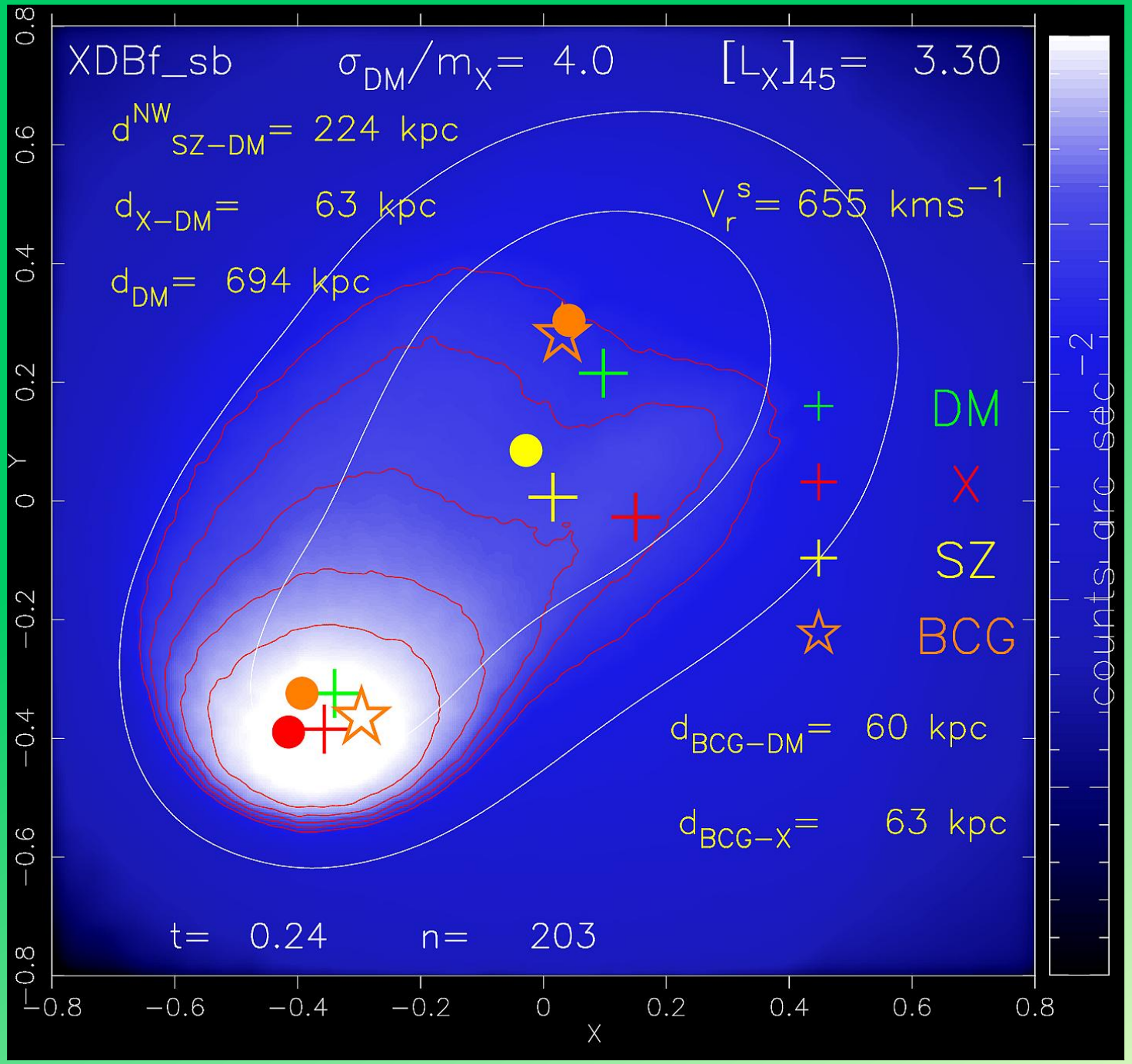
XDBf_sb
σ_{DM}/m_X= 4.0
$[L_X]_{45}$= 3.30
d^{NW}_{SZ-DM}= 224 kpc
d_{X-DM}= 63 kpc
d_{DM}= 694 kpc
V_r^s= 655 kms^{-1}
DM
X
SZ
BCG
d_{BCG-DM}= 60 kpc
d_{BCG-X}= 63 kpc
t= 0.24
n= 203
counts arc sec^{-2}
X
Y
−0.8
−0.6
−0.4
−0.2
0
0.2
0.4
0.6
0.8

RESULTS FROM MODEL XDBf_sb ($\sigma_{DM} / m_X = 4cm^2 / gr$)

- The measured offsets between the different mass components are well reproduced by the SIDM merging model
- The damping of DM velocities also impact on BCGs : stellar bulk velocities are reduced as well because they now experience a drag force due to the DM , the relative mean bulk velocity V_r^s between the two BCGs along the line-of sight is now of the order of $\sim 600 km/s$: this value is quite close to that measured by Menanteau+12
- The X-ray emission in the wake behind the SE is weaker than in the σ_DM =0 model→ complex dynamical interplay between baryons and SIDM during the collision

OBSERVATIONAL CONSTRAINTS ON THE SIDM MODEL XDBf_sb

I: ESTIMATES OF THE X-RAY PEAK POSITIONAL ERROR

According to Kim+21 the null hypothesis of zero size offsets can be excluded with high significance

The positional error of the X-ray emission peak is expected to be very small, being set by the angular resolution of the Chandra X-ray image ($0.5''$)

The error in the estimate of the X-ray peak offset is then dominated by the WL uncertainty σ_{DM} and the offset is in the range

$$d^{SE}_{X-DM} \sim 100 \pm 40\,\mathrm{kpc}$$

This shows that simulations with $\sigma_{DM}/m_X \lesssim 2\,\mathrm{cm}^2\mathrm{gr}^{-1}$ are marginally inconsistent with the observed X-DM offset. For these merger models $d^{SE}_{X-DM} \lesssim 40\,\mathrm{kpc}$

We thus assume that SIDM merger models of El Gordo cluster with $\sigma_{DM}/m_X \sim 1\,\mathrm{cm}^2\mathrm{gr}^{-1}$, and thus with offsets $\Delta_{sim} \lesssim 50\,\mathrm{kpc}$, are disfavoured over $\sigma_{DM}/m_X \sim 4\,\mathrm{cm}^2\mathrm{gr}^{-1}$ models having $\Delta_{sim} \sim 70 - 100\,\mathrm{kpc}$

Note that as $\sigma_{DM}/m_X \to 0$ $\Delta_{sim} \to 0$ so that collisionless DM is ruled out at ~2σ level

II: MATCHING THE X-RAY MORPHOLOGY

The SIDM model that best matches the various offsets exhibits a very faint X-ray emission behind the SE peak. After the various tweaks we have attempted for the initial condition parameters, we found that this emission can be restored to observational levels by choosing $\{ \mathrm{M}_1,\ q,\ V,\ P\} = \{1.6 \cdot 10^{15}\,\mathrm{M}_\odot, 2.32, 700\,\mathrm{kpc}, 2,500\,\mathrm{km\ s}^{-1}\}$ and $\{ \mathrm{f}_{g1}, f_{g2}\} = \{0.16, 0.16\}$

However, as a side effect of these settings, the final L_X blows up by a factor ~ 3

Because the bulk of L_X comes from the X-ray peak, L_X can be reduced by increasing the size of the SE inner cool core. However, this choice comes at the price of a negative d^{SE}_{X-DM} , with the X-ray peak now behind the DM centroid

This is because the gas density peak is now much less concentrated and experiences a significantly larger ram pressure force from the ICM of the primary

III: CONTRAINTS ON DM HALO PROFILES FROM WEAK LENSING

- In accord with SIDM predictions, at inner radii the post collision cluster DM density profiles are cored. These profiles are well fitted using a Burkert profile with core radius $\sim 300\,\mathrm{kpc}$

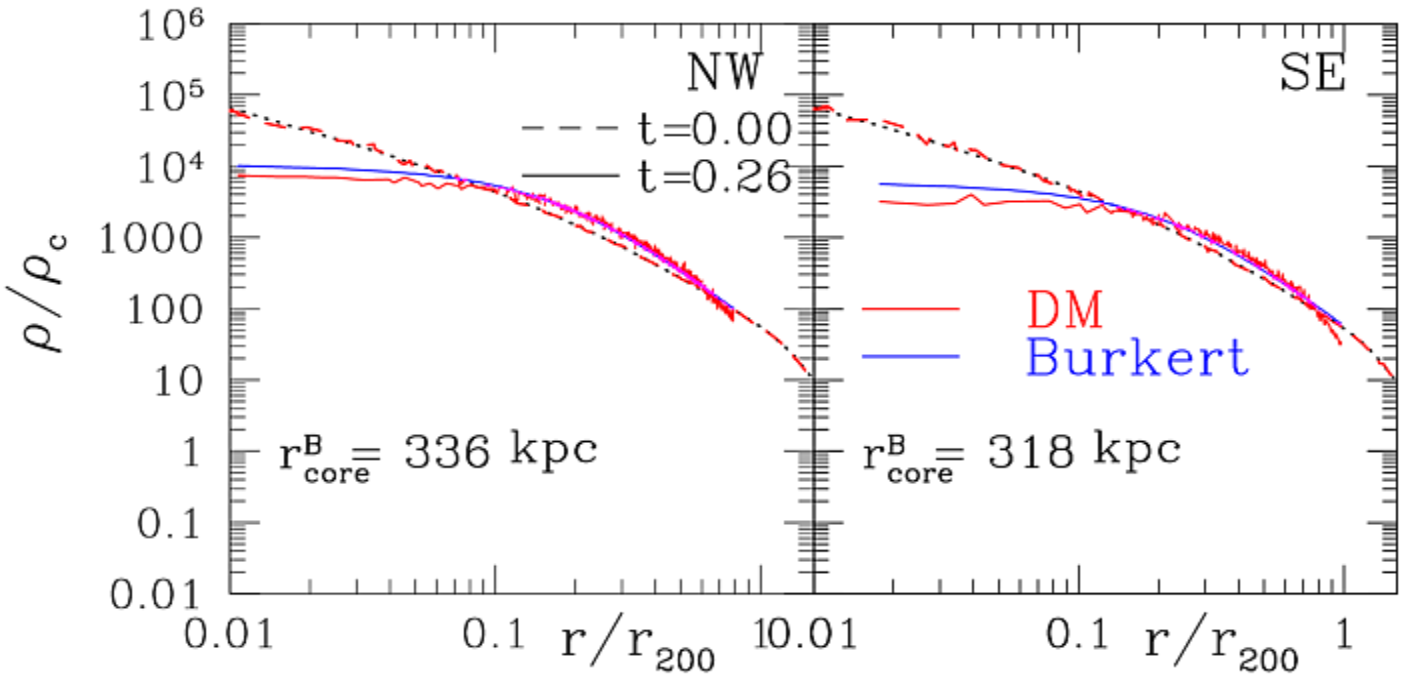

Measured radial density profiles of the two DM halos of the merger model XDBf_sb. The left (right) panel is for the NW (SE) cluster. Solid red lines refer to the present epoch, when the projected separation between the mass centroids of the two components is approximately $d_{DM} \sim 700$, and dashed red lines correspond to the start of the simulation at $t = 0$. The origin of the profiles is centered on the position of the mass centroid. For each cluster an NFW density profile is used to fit the DM density profile at $t = 0$ (black dot line), while in order to fit the cored DM profile at $t = 0.26$ Gyr we adopted a Burkert profile (solid blue line). In each panel is reported the value of the corresponding core radius r^B_{200}, the related statistical error being negligible.

Can we put constraints on these profiles from weak lensing studies of El Gordo ?

In the weak lensing regime two fundamental quantities are

$$\begin{cases} g_T = \textit{reduced tangential shear} & = & \frac{\gamma_+}{1-\kappa} \\ \gamma_+ = \textit{averaged tangential shear} & \equiv & \frac{\Delta\Sigma}{\Sigma_c} \end{cases}$$

These can be predicted at the projected radius R from the l.o.s. surface mass density

$$\begin{cases} \Sigma(R) & = & \int_{-\infty}^{\infty} \rho(\sqrt{R^2+\chi^2})d\chi \\ \overline{\Sigma}(R) & = & \frac{2}{R^2}\int_0^R \Sigma(R')R'dR' \\ \Delta\Sigma(R) & = & \overline{\Sigma}(R) - \Sigma(R) \end{cases}$$

where $\kappa = \Sigma(R)/\Sigma_c$ and $\Sigma_c = \frac{c^2}{4\pi G}\frac{D_s}{D_d D_{ds}}$

From the fiducial best-fit DM profiles one can construct the reduced tangential shear profiles $g_T(R)$ and compare them with measured profiles (Jee+14, Kim+21)

$$\begin{cases} \Sigma_B(R) &= 2r_c\rho_0 \int_0^\infty \frac{dz'}{(1+s)(1+s^2)} \\ &\equiv 2r_c\rho_0 I(u) \\ I(u) &\simeq \frac{\pi}{4}\frac{1}{1+u^2} \end{cases} \qquad s^2 = z'^2 + u^2,\ z' = z/r_c \ and \ u = R/r_c$$

In the following plots, for each cluster we show the lensing profiles $g_T^{Burk}(\theta)$, as calculated from the corresponding best-fit halo Burkert profiles.
For completeness, we also show the NFW lensing profiles $g_T^{NFW}(\theta)[\sigma_{DM} = 0]$, as derived from a standard CDM run

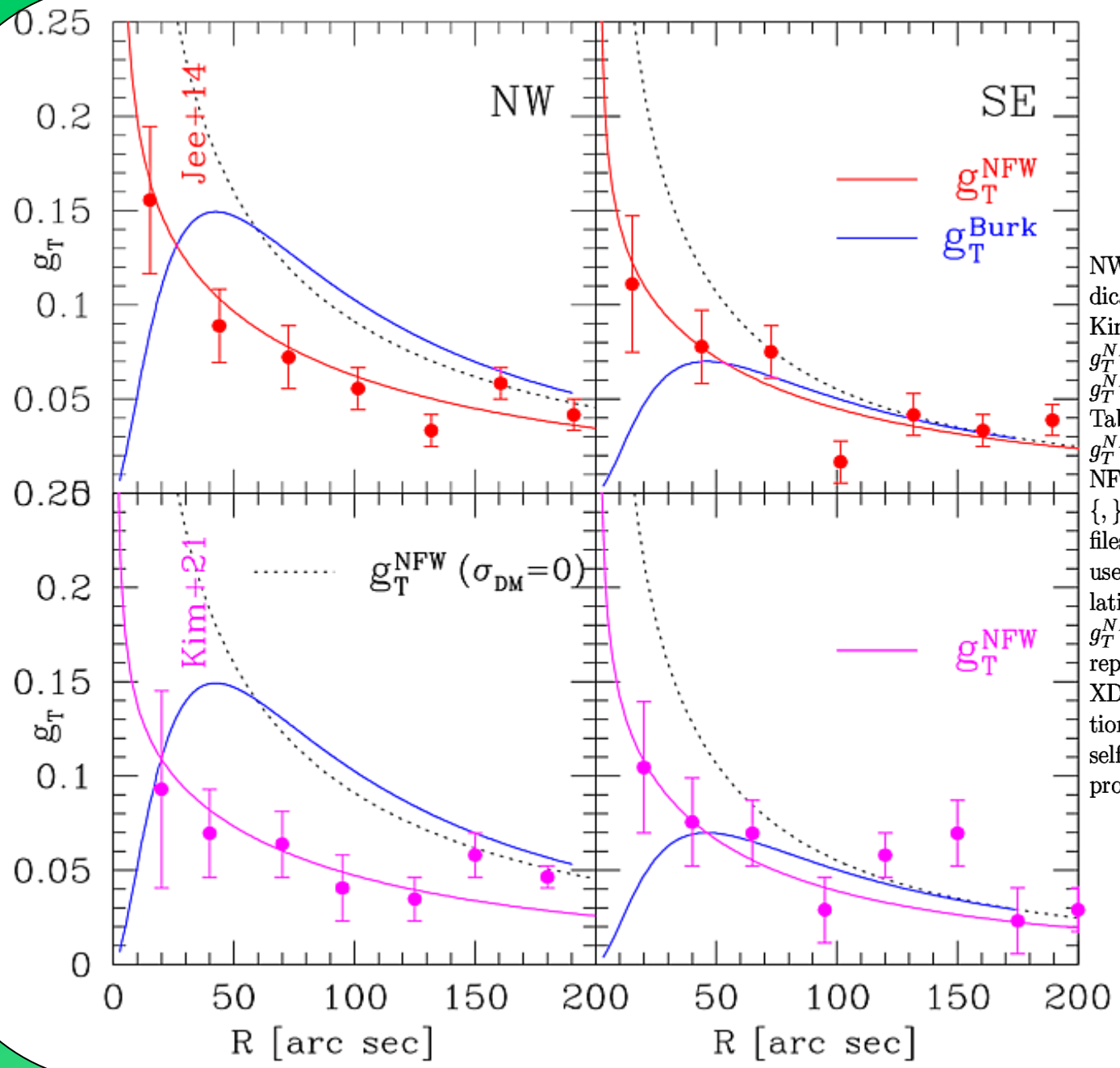

Left (right) panels show the reduced tangential shear profiles $g_T(\theta)$ for the NW (SE) cluster, as measured by some authors. Top and bottom panels indicate the data points as extracted from Figure 9 of Jee14 and Figure 17 of Kim21, respectively. In each panel the data points are compared against a $g_T^{NFW}(\theta)$ profile as obtained by a NFW mass model. For the top panels the $g_T^{NFW}(\theta)$ profiles are constructed using the best-fit NFW parameters taken from Table 2 of Jee14: $\{r_{200}^{NW}, r_{200}^{SE}\} = \{1.65, 1.38\}$. and $\{,\} = \{2.57, 2.65\}$. The $g_T^{NFW}(\theta)$ profiles shown in the bottom panels are computed according to the NFW parameters reported in Table 2 of Kim21: $\{r_{200}^{NW}, r_{200}^{SE}\} = \{1.5, 1.3\}$ and $\{,\} = \{2.54, 3.20\}$. Solid blue lines refer to the reduced tangential shear profiles $g_T^{Burk}(\theta)$, these have been inferred from the best-fit Burkert density profiles used to model the cored DM profiles extracted from the SIDM merging simulation XDBf_sb. The black dot lines correspond to the NFW lensing profiles $g_T^{NFW}(\theta)[\sigma_{DM} = 0]$. These were derived from an NFW density model used to reproduce the final halo DM density profiles of a mirror simulation of model XDBf_sb. The simulation was performed by adopting the same initial condition setup of the SIDM merging run XDBf_sb, but without allowing DM to be self-interacting by setting $\sigma_{DM}/m_X = 0$. The NFW parameters of the density profiles are $\{r_{200}^{NW}, r_{200}^{SE}\} = \{1.84, 1.38\}$ and $\{,\} = \{3.97, 5.0\}$, respectively.

The profiles show that the size of the DM core radii predicted by the SIDM simulation are too large ($\sim 200 \quad kpc$) to be consistent with the measured values of $g_T(R)$ in the innermost bins

This inconsistency implies for the DM a very odd behavior during the merger: The DM behaves collisionless as far as it concerns the internal motion within each halo, but it appears to be self-interacting when one considers the relative bulk motion between the two cluster DM halos

to summarize ....

MAIN BENEFITS AND DRAWBACKS OF AN SIDM MODEL FOR THE EL GORDO CLUSTER

- ✓ A SIDM merger model with $\sigma_{DM}/m_X \simeq 4\,\mathrm{cm}^2\mathrm{gr}^{-1}$ can match all of the observed offsets : DM-X , DM-BCG for the SE cluster, and DM-SZ for the NW cluster

-This is highly non-trivial because the model can account of all the measured offsets simultaneously (unlike as in standard CDM)

- ✓ The relative mean bulk velocity V_r^s along the line-of-sight between the two BCGs is now in much better agreement with data , this is because in SIDM the BCGs now experience a drag force due to the interacting DM

ON THE OTHER HAND...

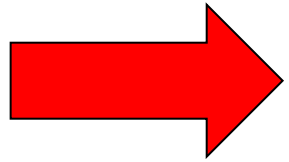

✓ The twin-tailed X_ray morphology is not well reproduced because of its reduced resiliency in the much shallower DM potential wells

- Increasing the gas fractions does not solve the problem because the DM-X offset tends in turn to negative values due to ram-pressure effects

✓ The best match to the data is obtained for a SIDM model with $\sigma_{DM}/m_X \simeq 4-5\,\mathrm{cm^2 gr^{-1}}$

- Such values are largely inconsistent with present upper limits ($\lesssim 1\,\mathrm{cm^2 gr^{-1}}$) at cluster scales (Kim+17, ….)

- To resolve this tension we suggest the possibility that DM interactions come into play according to some energy level of the cluster collision

✓ Finally, the most significant drawback is the tension at small-angles between the measured lensing profiles $g_T(\theta)$ and the corresponding profiles derived from the SIDM merging simulation

BY PUTTING ALL OF THIS TOGETHER…

THERE IS NO EASY WAY ……

These difficulties to match simultaneosly all of the observational constraints for the El Gordo cluster are suggestive of non-trivial DM physics and that the description of DM self-interactions based on the scattering of DM particles is too simplistic to account of the overall El Gordo phenomenology

To summarize, the SIDM theoretical motivated model used here should be considered as only a low order approximation of the far more complex underlying physical processes that describe DM interactions in major cluster mergers

We argue that such contradictions cannot be easily reconciled within the DM models presented so far in alternative to the collisionless paradigm. We suggest, however, that these tensions can be used as unique test bed to probe DM physics